Botulinum Toxin Potentiates Cancer Radiotherapy and Chemotherapy

Réginald Ansiaux,[1] Christine Baudelet,[1,2] Greg O. Cron,[1] Jérôme Segers,[1,2] Chantal Dessy,[3] Philippe Martinive,[3] Julie De Wever,[3] Julien Verrax,[5] Valérie Wauthier,[5] Nelson Beghein,[1,2] Vincent Grégoire,[5] Pedro Buc Calderon,[5] Olivier Feron,[3] and Bernard Gallez[1,2]

Abstract

Purpose: Structural and functional abnormalities in the tumor vascular network are considered factors of resistance of solid tumors to cytotoxic treatments. To increase the efficacy of anticancer treatments, efforts must be made to find new strategies for transiently opening the tumor vascular bed to alleviate tumor hypoxia (source of resistance to radiotherapy) and improve the delivery of chemotherapeutic agents. We hypothesized that *Botulinum neurotoxin* type A (BoNT-A) could interfere with neurotransmitter release at the perivascular sympathetic varicosities, leading to inhibition of the neurogenic contractions of tumor vessels and therefore improving tumor perfusion and oxygenation.

Experimental Design: To test this hypothesis, BoNT-A was injected locally into mouse tumors (fibrosarcoma FSaII, hepatocarcinoma transplantable liver tumor), and electron paramagnetic resonance oximetry was used to monitor pO_2 *in vivo* repeatedly for 4 days. Additionally, contrast-enhanced magnetic resonance imaging was used to measure tumor perfusion *in vivo*. Finally, isolated arteries were mounted in wire myograph to monitor specifically the neurogenic tone developed by arterioles that were co-opted by the surrounding growing tumor cells.

Results: Using these tumor models, we showed that local administration of BoNT-A (two sites; dose, 29 units/kg) substantially increases tumor oxygenation and perfusion, leading to a substantial improvement in the tumor response to radiotherapy (20 Gy of 250-kV radiation) and chemotherapy (cyclophosphamide, 50 mg/kg). This observed therapeutic gain results from an opening of the tumor vascular bed by BoNT-A because we showed that BoNT-A could inhibit neurogenic tone in the tumor vasculature.

Conclusions: The opening of the vascular bed induced by BoNT-A offers a way to significantly increase the response of tumors to radiotherapy and chemotherapy.

The tumor vascular network is the target of many advanced anticancer strategies, with two seemingly contradictory approaches (1). Therapies are designed to destroy the tumor vasculature, thereby depriving the tumor of oxygen and nutrients (2): these strategies use anti–vascular-targeting agents (3) and antiangiogenic agents (4). The major difference between antiangiogenic and vascular-targeting agents is that the latter are directed at the preexisting tumor vasculature, whereas the former are designed to affect the process of development. In contrast to previous strategies, the goal of the "provascular" approaches is to increase tumor perfusion and oxygenation temporarily through pharmacologic interventions. For this latter approach, radiotherapy could benefit from tumor reoxygenation because oxygen is a key factor in the response to irradiation (5). Additionally, a decrease in tumor interstitial pressure (6) or a normalization of the tumor vasculature at the early phase of an antiangiogenic treatment (7–9) could facilitate tumor accessibility to circulating chemotherapeutic drugs. Although such strategies seem rather simple, their implementation is not straightforward, because it is generally thought that structural and functional abnormalities of the immature tumor vessels could confer resistance to the relaxing properties of classic vasoactive drugs. Therefore, there is a real need for developing ways of transiently opening the tumor vascular bed to alleviate tumor hypoxia and increase the efficacy of anticancer cytotoxic therapies. In this study, we explored the role of Botulinum neurotoxin type A (BoNT-A) as a promising adjuvant to anticancer therapies.

Authors' Affiliations: Laboratories of [1]Biomedical Magnetic Resonance, [2]Medicinal Chemistry and Radiopharmacy, [3]Pharmacology and Therapeutics, and [4]Molecular Imaging and Experimental Radiotherapy; [5]Pharmacokinetic, Metabolism, Nutrition and Toxicology Unit, Université Catholique de Louvain, Brussels, Belgium

Received 6/7/05; revised 10/5/05; accepted 12/14/05.

Grant support: Belgian National Fund for Scientific Research grant 7.4503.02, the Fonds Joseph Maisin, and the Actions de Recherches Concertées/Communauté française de Belgique.

The costs of publication of this article were defrayed in part by the payment of page charges. This article must therefore be hereby marked *advertisement* in accordance with 18 U.S.C. Section 1734 solely to indicate this fact.

Note: R. Ansiaux is a Belgian National Fund for Scientific Research-Televie fellow. C. Baudelet is Scientific Research worker of the Belgian National Fund for Scientific Research. C. Dessy and O. Feron are Research Associates of the Belgian National Fund for Scientific Research.

Requests for reprints: Bernard Gallez, CMFA/REMA Units, Université Catholique de Louvain, Avenue E. Mounier 73.40, B-1200 Brussels, Belgium. Phone: 32-2-7642792; Fax: 32-2-7642790; E-mail: Gallez@cmfa.ucl.ac.be.

doi:10.1158/1078-0432.CCR-05-1222

BoNT-A has a wide variety of clinical indications, particularly for treating intractable muscle hyperactivity associated with strabismus, spasticity, hemifacial spasm, and blepharospasm (10). BoNT-A is largely known by the public for its cosmetic uses to rejuvenate the aging face. The Botulinum toxin is a neurotoxin composed of two polypeptide chains held together by a single disulfide bridge. The toxin works locally at the injection site and acts on neurotransmitter-mediated processes by blocking their release. Its mechanism consists of a metalloprotease activity against the synaptosomal-associated protein of 25 kDa (SNAP-25), which prevents the formation of the soluble *N*-ethylmaleimide-sensitive factor attachment protein receptor complex involved in the fusion of vesicles with presynaptic membranes and consequently impedes the release of neurotransmitters, such as acetylcholine and noradrenaline, at the neuromuscular junction (10–12). Thus far, there has been no investigation into the possible usefulness of BoNT-A as an adjuvant to cancer therapies. Our data present a paradigm according to which BoNT-A could interfere with neurotransmitter release at the perivascular sympathetic varicosities, leading to inhibition of neurogenic contractions of tumor vessels and therefore improving tumor perfusion and oxygenation. To characterize the changes in the tumor microenvironment induced by BoNT-A, we used several powerful tools: contrast-enhanced magnetic resonance imaging (MRI) has been used to measure tumor perfusion noninvasively (13); electron paramagnetic resonance (EPR) oximetry has made it now possible to monitor pO_2 *in vivo* repeatedly and relatively noninvasively (14, 15); and myograph setup has been used to study the particular reactivity of arterioles co-opted by the tumor. We showed a substantial increase in tumor perfusion and oxygenation after BoNT-A administration, which led to a substantial improvement in the response of tumors to radiotherapy and chemotherapy.

Material and Methods

Experimental animals and tumors

Two different tumor models were implanted in the thigh of mice: a Syngeneic FSa II fibrosarcoma model (16) in C3H/HeOuJIco mice and a transplantable mouse liver tumor model (17) in NMRI mice. Both tumor models were previously characterized in our group for assessing the effect of treatments that potentiate radiotherapy (18) and chemotherapy.[6] Tumors were measured daily with an electronic caliper. For all experiments, tumor-bearing mice were anesthetized using isoflurane (2.5% for induction, 1% for maintenance). All animal experiments were conducted in accordance with national animal care regulations.

BoNT-A preparation and injection procedure

BoNT-A solution in saline (Botox, Allergan, Antwerp, Belgium) or saline solution (control) was injected when tumors reached a diameter of 6.7 ± 0.2 mm. BoNT-A was administered in the tumor at two different sites (two injections of 20 μL, corresponding to a total dose of 29 units/kg).

Tumor oxygenation

EPR Oximetry, using charcoal (CX0670-1, EM Science, Gibbstown, NJ) as the oxygen sensitive probe, was used to evaluate the tumor oxygenation (14). EPR spectra were recorded using an EPR spectrometer (Magnettech, Berlin, Germany) with a low-frequency microwave bridge operating at 1.2 GHz and extended loop resonator. Mice were injected in the center of the tumor 1 day before measurement using the suspension of charcoal (suspension in saline containing 3% Arabic gum, 100 mg/mL, 50 μL injected, 1-25 μmol/L particle size). The localized EPR measurements correspond to an average of pO_2 values in a volume of ~10 mm^3 (14). To avoid any acute effect of the treatment, data acquisition was made before the injection of BoNT-A or saline and then on a daily basis.

Flow and permeability measurements

Patent Blue staining. Patent Blue (Sigma-Aldrich, Bornem, Belgium) was used to obtain a rough estimate of the tumor perfusion (8) 3 days after administration of BoNT-A or vehicle. This technique involves the injection of 200 μL of Patent Blue (1.25%) solution into the tail vein of the mice. After 1 minute, a uniform distribution of the staining through the body was obtained, and mice were sacrificed. Tumors were carefully excised and cut in two size-matched halves. Pictures of each tumor cross-section were taken with a digital camera. To compare the stained versus unstained area, an in house program running on IDL (Interactive Data Language, RSI, Boulder, CO) was developed. For each tumor, a region of interest (stained area) was defined on the two pictures, and the percentage of stained area of the whole cross-section was determined. The mean of the percentage of the two pictures was then calculated and was used as an indicator of tumor perfusion.

Dynamic contrast enhanced MRI. The perfusion was monitored on day 3 after injection of BoNT-A ($n = 3$) or saline ($n = 4$) via single-slice dynamic contrast-enhanced MRI at 4.7 T using the rapid clearance blood pool agent P792 (Vistarem, Guerbet, Roissy, France; ref. 19). High-resolution multislice T_2-weighed spin echo anatomic imaging was done just before dynamic contrast-enhanced imaging. Pixel-by-pixel values for K^{trans} (influx volume transfer constant, from plasma into the interstitial space, units of min^{-1}), V_p (blood plasma volume per unit volume of tissue, unitless), and K_{ep} (fractional rate of efflux from the interstitial space back to blood, units of min^{-1}) in tumor were calculated via tracer kinetic modeling of the dynamic contrast-enhanced data (19), and the resulting parametric maps for K^{trans}, V_p, and K_{ep}, were generated. Statistical significance for V_p or K^{trans} identified "perfused" pixels (i.e., pixels to which the contrast agent P792 had access; refs. 19, 20).

Miles assay. The Evans blue technique was used to measure the tumor vasopermeability to macromolecules. This technique provides a good estimate of the extravasation and interstitial accumulation of albumin (21) as Evans blue dye makes a complex with the negatively charged intravascular albumin by electrostatic combination. Briefly, Evans blue (2.5 mg/mL in NaCl 0.9%) was administered i.v. (10 mg/kg) in control and treated mice. The dye was allowed to circulate for 1 hour before sacrifice of the animals. Tumors were then excised, weighed, and put in formamide (2 mL/tumor) for 24 hours at 55°C for Evans blue extraction. The Evans blue concentrations were determined by spectrophotometry at 620 nm and expressed in terms of concentration per gram of tumor tissue.

Irradiation and tumor regrowth delay assay

The FSaII tumor-bearing leg was locally irradiated with 20 Gy of 250-kV X-rays (RT 250; Philips Medical Systems, Andover, MA). The tumor was centered in a 3-cm diameter circular irradiation field. A single dose irradiation of 20 Gy, 3 days after the i.t. injection of BoNT-A, was done. After treatment, the tumor growth was determined daily by measuring transversal and anteroposterior tumor diameters until they doubled in size, at which time the mice were sacrificed. A linear fit was done between 8 and 16 mm, which allowed determination of the time to reach a particular size for each mouse.

Chemotherapy and tumor regrowth delay assay

BoNT-A–treated mice received a single dose (50 mg/kg via 100 μL i.p.) of cyclophosphamide, an alkylating agent. Regrowth delay

[6] P. Martinive, submitted for publication.

experiments in transplantable liver tumor have shown that this dose of 50 mg/kg is just below the efficacy threshold for this product (experiments done with dose range of 250-10 mg/kg).

Clonogenicity assay

FSAII tumors in mice were dissected in a sterile environment and gently pieced in McCoy's medium. The cell suspension was filtered (100-μm-sized pore nylon filter, Millipore, Brussels, Belgium) and centrifuged (5 minutes, 450 × *g*, 4°C), and cells were set to culture in DMEM containing 10% fetal bovine serum. Confluent cells were treated with BoNT-A (0.73 units/10^8 cells) 4 hours before being irradiated at 2 Gy. To assess the cell radiosensitivity, trypan blue exclusion dye method and a clonogenic cell survival assay were done. For the former, the cells were counted for viability 24 hours after irradiation. For the latter, the cells were washed and reincubated in the conditioned medium without drug 24 hours after irradiation. After a 7-day incubation in a humidified 5% CO_2 atmosphere at 37°C, the dishes were stained with crystal violet, and colonies with >50 cells were counted. The experiments were carried out in triplicate.

Apoptotic activity

The apoptotic activity inside tumors was assessed by measuring the activity of caspase-3, a well-known effector involved in the apoptosis induced by chemotherapeutic or radiotherapeutic treatments. The activation of caspase-3 was measured by immunoblotting, and the results were confirmed by measuring the cleavage of poly(ADP-ribose) polymerase, a polypeptide cleaved during apoptosis process. Tumors were dissected, minced, put in an extraction buffer solution [10 mmol/L Tris, 1 mmol/L EDTA, 250 mmol/L sucrose, 0.1 mmol/L phenylmethylsulfonyl fluoride, 10 mmol/L NaF, 1 mmol/L Na_3VO_4, supplemented with protease inhibitor cocktail (Complete Mini, Roche Applied Science, Mannheim, Germany; pH 7.4] and homogenized with a Potter-Elvehjem tissue grinder. The tumor homogenates were centrifuged at 10,000 × *g* for 20 minutes, and the supernatant fraction was saved for analysis. From these homogenates, protein concentration was determined by the Bradford protein assay (22). Equal amounts of proteins (50 μg) were subjected to SDS-PAGE [6% and 15% separating gels, respectively, for poly(ADP-ribose) polymerase and caspase-3 detection] followed by electroblot to nitrocellulose membranes. The membranes were blocked 1 hour in TBS buffer (pH 7.4) containing 5% powdered milk protein followed by an incubation of 2 hours with diluted antibodies in a fresh solution of powdered milk protein (1% w/v in TBS buffer). The membranes were washed and incubated for 60 minutes with a dilution of secondary antibody coupled with horseradish peroxidase. Anti-poly(ADP-ribose) polymerase and anti-caspase-3 rabbit polyclonal antibodies were diluted by 1:200 and goat anti-rabbit polyclonal antibody by 1:10 000. They were purchased respectively from Santa Cruz Biotechnology (Santa Cruz, CA) and Chemicon, Inc. (Temecula, CA). The quantification of the Western blot bands was done with by densitometry (Image Master V1.1, Pharmacia Biotech, Piscataway, NJ).

Myogenic tone measurements

Segments of the co-opted saphenous arteries (±2 mm in length) were carefully dissected. For each tumor, two adjacent segments were mounted in a multiwire myograph (610M, DMT, Aarhus, Denmark). Briefly, two 40-μm wires were threaded through the lumen of the vessel segment. One wire was attached to a stationary support driven by a micrometer, whereas the other was attached to an isometric force transducer. The bath of the myograph was filled with physiologic salt solution [120 mmol/L NaCl, 5.9 mmol/L KCl, 25 mmol/L $NaHCO_3$, 17.5 mmol/L dextrose, 2.5 mmol/L $CaCl_2$, 1.2 mmol/L $MgCl_2$, 1.2 mmol/L NaH_2PO_4 (pH 7.4)], gassed, and maintained at 37°C. After mounting, vessels were maintained under zero force for 45 to 60 minutes. A passive diameter-tension curve was constructed. The vessel was set at a tension equivalent to that generated at 90% of the diameter of the vessel under a transmural pressure of 100 mm Hg. The viability of the vessels was assessed by measuring the contractile response to a depolarizing solution (physiologic salt solution where 100 mmol/L KCl replaced NaCl stoichiometrically). After washing, the vessels (n = 4) were incubated in the presence of BoNT-A (0.12 unit/mL) for 2 hours, whereas the matched controls (adjacent segments) were kept in physiologic salt solution + solvent. All vessels were then challenged with a high KCl solution (40 mmol/L KCl) to depolarize smooth muscle cells of the media and nerve endings, thereby activating the Ca^{2+}-dependent release of neurotransmitter. The amplitude of the neurotransmitter release was estimated by measuring the relaxation to an α-adrenoceptor blocker (phentolamine) or to a cholinergic antagonist (atropine) for noradrenaline and acetylcholine, respectively.

Statistical analysis

Results are given as means ± SE from n animals. Comparisons between groups were made with Student's two-tailed t test or two-way ANOVA where appropriate, and $P < 0.05$ was considered significant.

Results

BoNT-A increases tumor oxygenation and perfusion. To determine the effect of BoNT-A on the tumor oxygenation as well as the kinetics of the effect, the partial pressure of oxygen (pO_2) was measured daily after i.t. injection of BoNT-A in two different sites. As shown in Fig. 1, the pO_2, which was very low in the FSaII tumors before the treatment (3.2 ± 0.5 mm Hg, n = 10), significantly increased after administration of BoNT-A, with a maximal pO_2 reached after 3 days (8.2 ± 1.6 mm Hg).

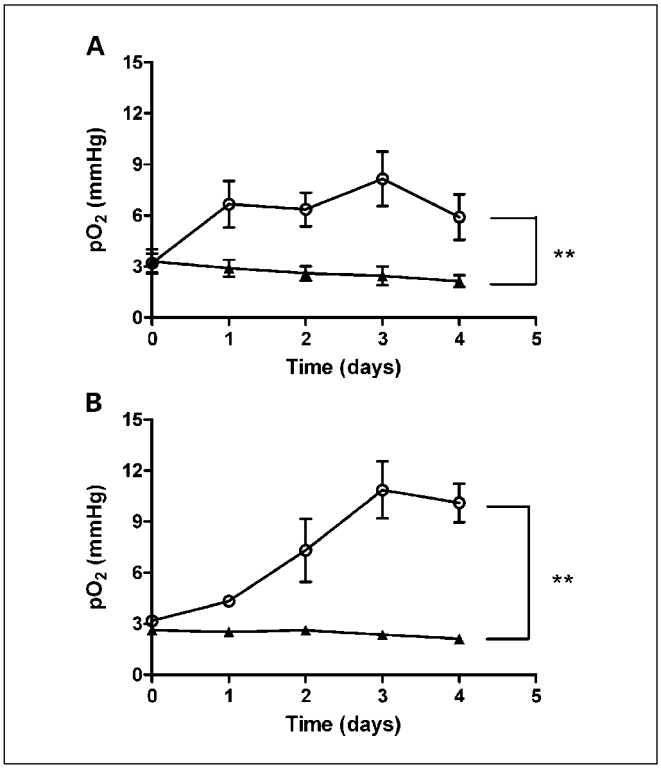

Fig. 1. Effect of a single i.t. injection of BoNT-A on FSAII tumor (*A*) and transplantable liver tumor (*B*) oxygenation monitored by EPR Oximetry. ▲, control group (n = 8 and 4 for FSAII and transplantable liver tumor, respectively). ○, treated group (n = 10 and 4 for FSAII and transplantable liver tumor, respectively). Note the significant increase in pO_2 24 hours after the injection with a maximum on day 3. Points, mean; bars, SE. **, $P < 0.01$.

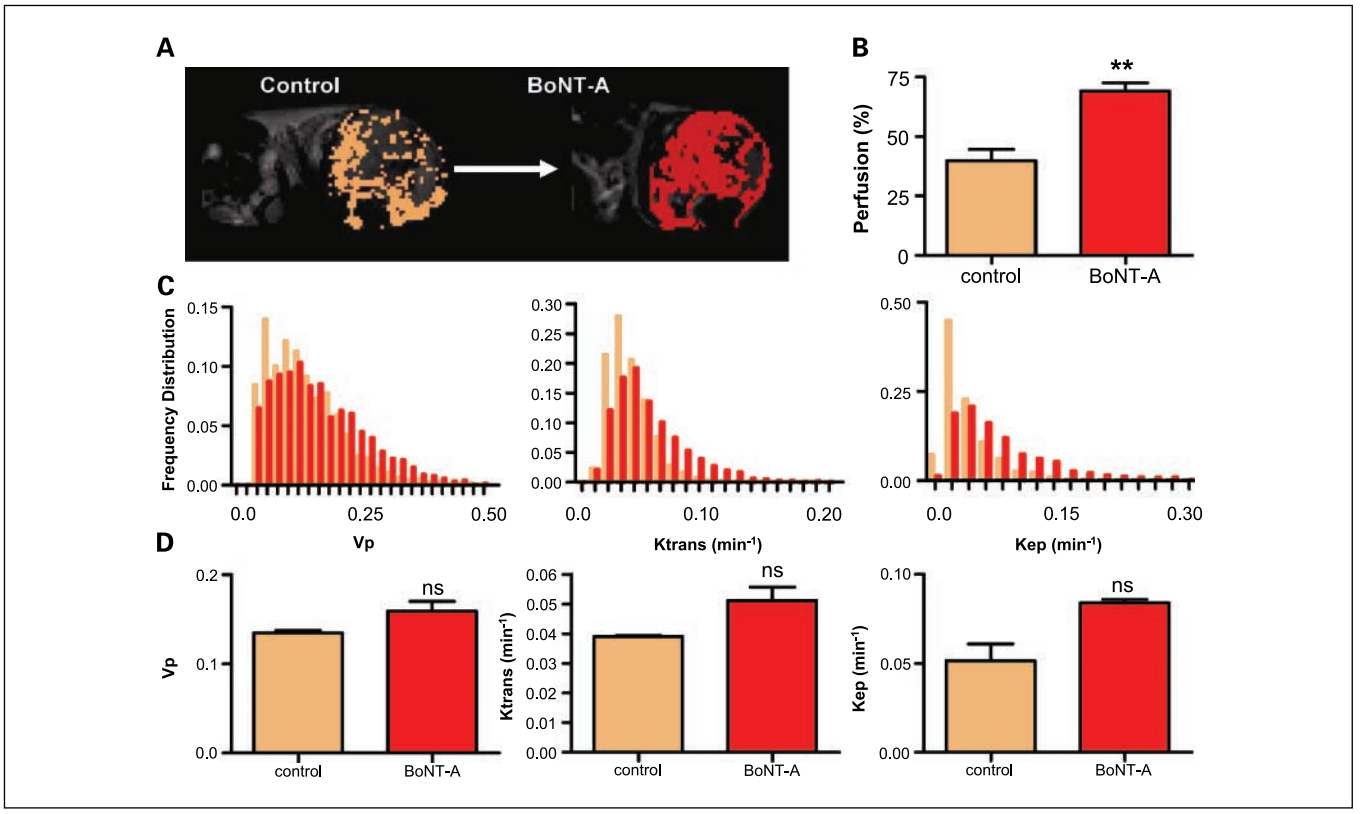

Fig. 2. *A,* typical MRI images of FSAll tumors showing the perfused pixels 3 days after treatment or vehicle. *B,* mean percentage of perfused pixels for treated ($n = 3$) and control group ($n = 4$). *C,* distribution of pharmacokinetics parameters in tumors treated with vehicle or BoNT-A. V_p is the blood plasma volume per unit volume of tissue. K^{trans} is the influx volume transfer constant from plasma into the interstitial space. K_{ep} is the efflux volume transfer constant from the interstitial space back to the plasma. *D,* overall estimation of pharmacokinetic parameters after BoNT-A treatment. Columns, mean; bars, SE. **, $P < 0.01$. ns, not significant.

The tumor pO_2 was found to be statistically different between BoNT-A–treated tumors and controls (two-way ANOVA). A similar effect was observed in transplantable liver tumors (10.9 ± 1.7 mm Hg on day 3 versus 3.2 ± 0.3 m Hg on day 0; $n = 4$). Therefore, all further experiments for the characterization of the tumor microenvironment and the establishment of the therapeutic relevance of the administration of BoTN-A were conducted on day 3.

Tumor perfusion was monitored in the FSaII tumor model on day 3 after BoNT-A administration via dynamic contrast-enhanced MRI at 4.7 T using i.v. injection of the rapid-clearance blood pool agent P792 (Vistarem; ref. 19). The pixel-by-pixel analysis generated "perfusion maps" (using the values for V_p), and "permeability maps" (using the values for K^{trans} and K_{ep}). Moreover, the kinetics analysis identified "perfused pixels" (i.e., pixels to which the contrast agent had access, showing a statistical significance for V_p or K^{trans}; ref. 19). Figure 2A shows typical images in mice treated by BoNT-A or vehicle 3 days after i.t. administration. The fraction of perfused pixels for the tumors treated with BoNT-A (Fig. 2B) was significantly greater than that of controls (69.2 ± 3.4 %, $n = 3$ versus 39.9 ± 4.7 %, $n = 4$ respectively; $P < 0.05$, Student's t test). No differences in the average values of K^{trans}, K_{ep}, or V_p were observed between tumors treated with BoNT-A or vehicle (Fig. 2C-D). These results indicate that there are more areas of the tumor that are

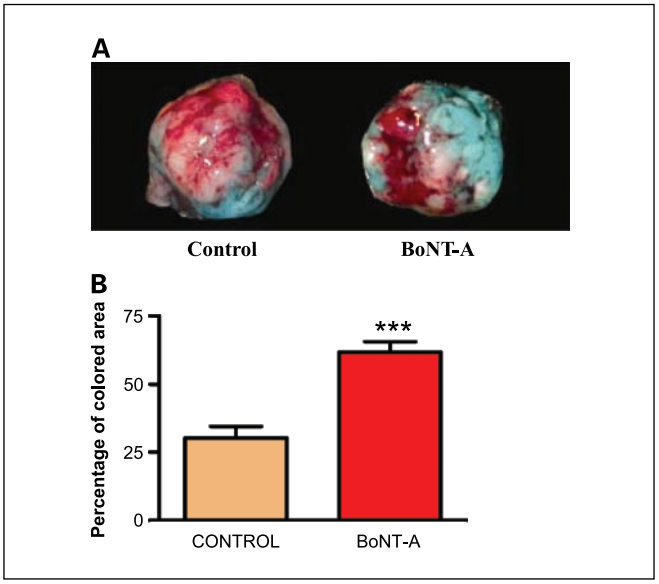

Fig. 3. *A,* typical images of FSAll tumors stained by the Patent blue 3 days after the injection of vehicle or BoNT-A. Note that the FSAll-treated tumor stained more positive than the control. *B,* effect of BoNT-A on tumor perfusion assessed by Patent blue staining 3 days after the single injection. Columns, mean value of tumor percentage of colored area for control group ($n = 5$) and treated group ($n = 8$). ***, $P < 0.001$.

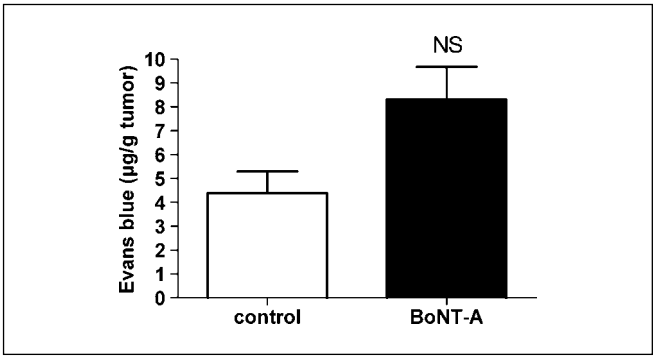

Fig. 4. Uptake of albumin-Evans blue in FSAll tumors. A nonsignificant increase is observed for treated groups (8.30 ± 1.38, $n = 4$ versus 4.38 ± 0.92 µg/g FSAll tumor, $n = 4$ for treated and control group, respectively). Columns, mean value of Evans blue uptake (µg/g tumor). ns, not significant.

perfused after BoNT-A treatment with no changes in hemodynamic variables. These results were further confirmed by a simple experiment in which a dye (Patent Blue) was administered by i.v. injection 1 minute before the sacrifice of the animal (8). After tumor excision and cutting two size-matched halves, the stained areas were digitally analyzed. Figure 3 shows typical images and quantitative data: tumors treated with BoNT-A stained more positive (61.7 ± 3.8%, $n = 8$) than control tumors (30.2 ± 4.4%, $n = 5$). The difference was found to be statistically significant ($P < 0.01$, unpaired t test). These results show the better accessibility of the dye when the tumor was pretreated by BoNT-A compared with controls. Finally, the Miles assay (Fig. 4) indicated that there was an increase in the uptake of albumin-Evans blue complex by treated tumors (8.30 ± 1.38 µg/g, $n = 4$) compared with control tumors (4.38 ± 0.92 µg/g, $n = 4$). However, this increase was not statistically significant ($P > 0.05$). These results are consistent with the dynamic contrast-enhanced MRI results (non significant increase of K^{trans}). The weak increase in permeability could be in part the result of the higher blood supply which may result in a higher Evans blue uptake (23).

BoNT-A increases the efficacy of radiotherapy and chemotherapy. To assess the therapeutic relevance of the previous findings (significant increase in tumor oxygenation and perfusion), we investigated the potentiation of radiation therapy and chemotherapy by BoNT-A. Figure 5 shows the tumor growth of FSaII tumors that receive injection of BoNT-A or vehicle, with or without irradiation at day 3 after administration (considered as day 0 on the irradiation graph). Interestingly, the administration of BoNT-A ($n = 6$) did not affect the tumor growth compared with the control group ($n = 5$). When irradiated (without BoNT-A) with 20 Gy of radiation, the tumor growth was delayed (regrowth delay for doubling the tumor size of 11.0 ± 0.2 days, $n = 5$). Pretreatment with BoNT-A led to a significant increase in the tumor regrowth delay (15.7 ± 1.0 days, $n = 6$). To discriminate between an oxygen effect and a direct radiosensitizing effect, the radiosensitivity was tested on FSAII cells in the presence of BoNT-A (Fig. 6). Compared with control cells, BoNT-A did not exert any sensitizing effect regardless of whether a trypan blue exclusion dye method (Fig. 6A) or clonogenic cell survival assay (Fig. 6B) was used. Meanwhile, the 2-Gy irradiation led to a significant decrease for both experiments. These observations show that BoNT-A radiosensitizes tumors through changes in the tumor microenvironment rather than by a direct sensitizing effect. We next evaluated the possible potentiation of chemotherapy by BoNT-A. Figure 7 shows the results from the experiment conducted on transplantable liver tumor pretreated by BoNT-A or the vehicle and receiving a suboptimal dose of cyclophosphamide (50 mg/kg) at day 3 after the treatment. In these conditions, the growth curves of the tumor did not differ, whereas the tumor growth was significantly delayed in tumors receiving the combination BoNT-A and cyclophosphamide. The regrowth delay for doubling the tumor size was 7.7 ± 0.4 and 11.7 ± 0.5 days for the groups receiving cyclophosphamide 3 days after administration of saline ($n = 7$) and BoNT-A ($n = 6$), respectively (significant difference, $P < 0.05$, unpaired t test). As expected, BoNT-A led to an increase in the apoptotic death associated with the radiotherapy and cyclophosphamide treatments. The activation of caspase-3 was 1.9 and 4.7 times increased when BoNT-A was associated with radiotherapy and chemotherapy, respectively (Fig. 8). Using BoNT-A alone (without radiotherapy or chemotherapy), we did not observe an activation of caspase-3 in these tumors. These results observed using caspase-3 were confirmed by an increase in the cleavage of poly(ADP-ribose) polymerase (data not shown).

BoNT-A interferes with neurogenic contractions of tumor vessels. In striated muscles, BoNT-A inhibits the release of the neurotransmitter acetylcholine at the neuromuscular junction, thereby interfering with striated muscle contractile tone. Similarly, we hypothesized that BoNT-A could interfere with neurotransmitter release at the perivascular sympathetic varicosities (24), leading to inhibition of tumor vessel neurogenic contractions and therefore improvement of tumor perfusion and oxygenation. To test this hypothesis, we used a model of isolated arteries mounted in wire myograph, which allowed us to monitor specifically the neurogenic tone developed by saphenous arterioles that were co-opted by the surrounding growing tumor cells. The vessels were challenged with a KCl solution to depolarize smooth muscle cells of the media and nerve endings, thereby also activating the Ca^{2+}-dependent release of neurotransmitter (25). The amplitude of

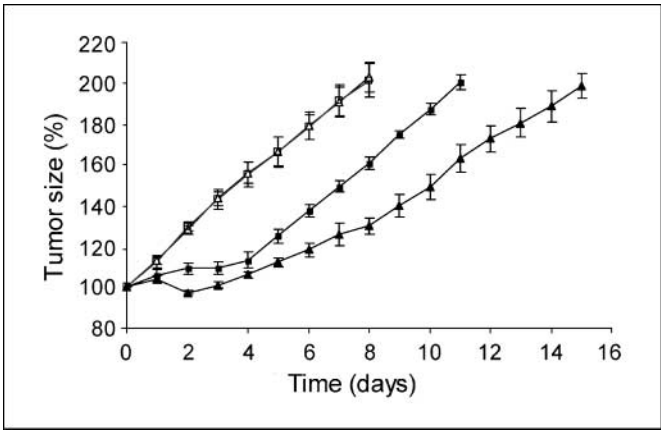

Fig. 5. Effect of the combination of BoNT-A and radiation on FSAll tumor regrowth. Mice were treated with BoTN-A (△; $n = 6$), treated with vehicle (□; $n = 5$), treated with 20 Gy of radiation 3 days after the injection of the vehicle (■; $n = 5$), or treated with 20 Gy of radiation 3 days after the injection of BoNT-A (▲; $n = 6$). Points, mean tumor size; bars, SE. Day 0 corresponds to the irradiation day. No difference in regrowth delay was observed between the control and treated groups alone. Regrowth delays to double tumor diameter were 11.04 ± 0.21 days for control + radiation and 15.70 ± 1.03 days for BoNT-A + radiation ($P < 0.01$). BoTN-A increased the regrowth delay by a factor 2.3.

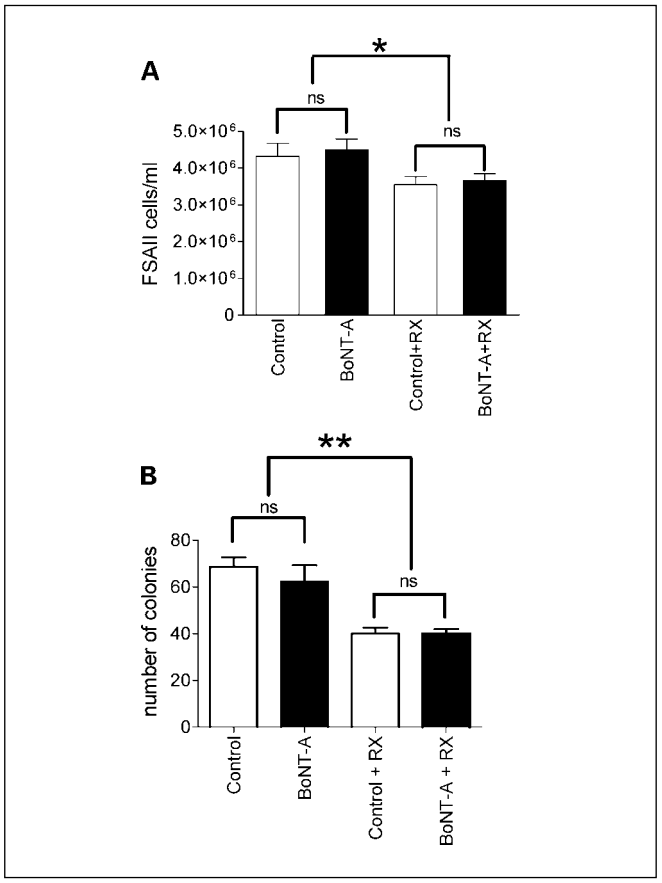

Fig. 6. Effect of BoNT-A (0.73 units/100 × 10^6 cells) on FSAII cells evaluated by the trypan blue exclusion dye method (*A*) and by the clonogenic cell survival assay (*B*). Both techniques showed an effect of the irradiation of 2 Gy on tumor cells. Nevertheless, BoNT-A did not exert any sensitizing effect regardless of the methods used. *, $P < 0.05$; **, $P < 0.01$; ns, not significant.

the neurotransmitter release was estimated by measuring the relaxation to an α-adrenoreceptor blocker (phentolamine) or to a cholinergic antagonist (atropine) for noradrenaline and acetycholine, respectively. We observed that in four vessels treated with BoNT-A, the relaxation to phentolamine was significantly smaller (52.4 ± 12.8% of the control) confirming that BoNT-A could interfere with the release of neurotransmitters (e.g., noradrenaline) and neurogenic vasoconstriction (Fig. 9). A similar experimental protocol using atropine failed to reveal a neurogenic acetylcholine-evoked contraction.

Discussion

The three major findings of this study are that (*a*) the use of local administration of BoNT-A can significantly promote tumor perfusion and oxygenation; (*b*) BoNT-A interferes with the vasoreactivity of vessels, particularly with the release of noradrenaline in arterioles co-opted by the surrounding tumor; and more importantly, (*c*) BoNT-A can increase the effectiveness of both tumor radiotherapy and chemotherapy.

For the first time, using an experimental model dedicated to the study of the functionality of isolated vessels, we have shown that BoNT-A can modulate the vasoreactivity of vessels feeding tumors. This unique information should be evaluated in the context of the vascular architecture of tumors. As emphasized in the introduction, hastily formed immature tumor microvessels lack smooth muscle layers and are less sensitive to vasomodulations. However, it is not uncommon to find mature blood vessels with smooth muscle layers and neural junctions inside slowly growing tumors (1). It was previously confirmed that these arterioles remain sensitive to vasomodulation under tumor co-option but also are subject to major adaptations to the tumor microenvironment (26, 27). Here, we found that BoNT-A inhibits the release of noradrenaline, a major endogenous vasomodulator that is responsible for the maintained sympathetic vascular tone through activation of vascular smooth muscle α-adrenoceptors. This is consistent with the opening of the tumor vascular bed that we observed *in vivo*. Even if we did not show an effect on the release of acetylcholine, we certainly cannot exclude such an effect. The lack of observation of this effect could result from the sparse cholinergic vascular innervation, the relatively short life of acetylcholine (rapidly destroyed by acetylcholine-esterase on its way from the synapse to the smooth muscle media) and/or from the relatively small number of muscarinic receptors present on the media. Overall, the effect on the release of neurotransmitters was sufficient to produce significant changes in the hemodynamics of the tumors.

The consequences of the modulations in the vasoreactivity of tumor vessels were remarkable in two ways. First, the accessibility of xenobiotics to the tumor was increased, as shown by the dynamic contrast-enhanced MRI study as well as

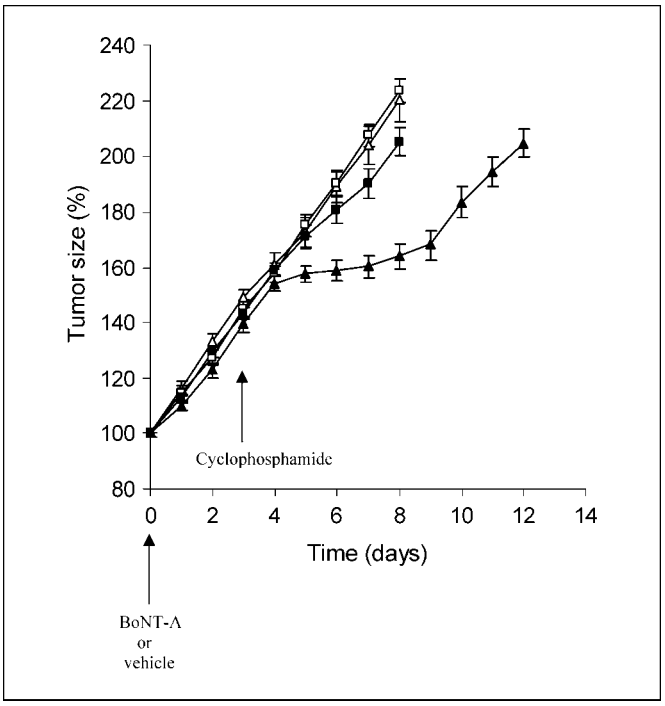

Fig. 7. Effect of the combination of BoNT-A and chemotherapy on transplantable liver tumor regrowth. Mice were treated with BoTN-A (△; $n = 8$), treated with vehicle (□; $n = 8$), treated with cyclophosphamide 3 days after the injection of the vehicle (■; $n = 7$), or treated with cyclophosphamide 3 days after the injection of BoNT-A (▲; $n = 6$). Point, mean tumor size; bars, SE. The injection of BoNT-A or vehicle was done on day 0. No difference in regrowth delay was observed among control, BoNT-A, and vehicle + cyclophosphamide groups. Regrowth delays to double tumor diameter were 7.73 ± 0.38 days for vehicle + cyclophosphamide and 11.68 ± 0.46 days for BoNT-A + cyclophosphamide ($P < 0.001$). BoTN-A increased the regrowth delay by a factor 5.1.

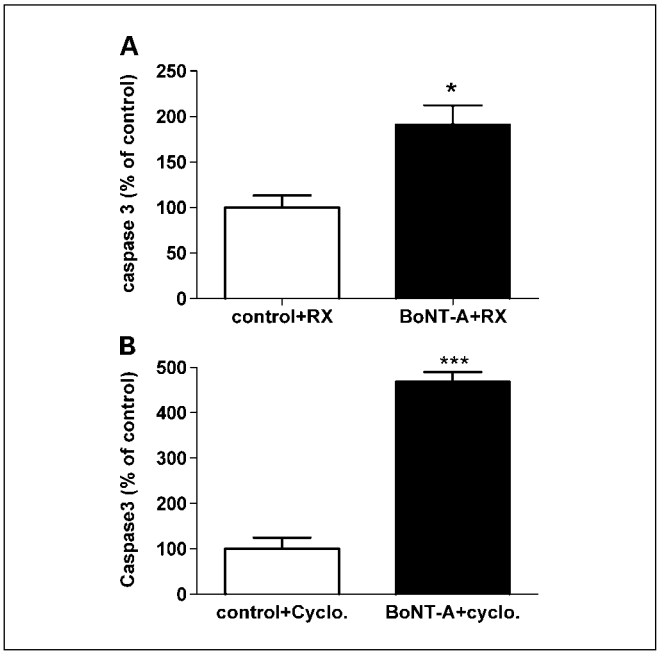

Fig. 8. Effect of BoNT-A on the caspase-3 activation. Percentage of control. Note the increase in the activation for BoNT-A treated mice when combined treatment is applied [1.9-fold increase with radiotherapy (*A*) and 4.7 fold increase with chemotherapy (*B*)]. Columns, % control; bars, SE. *, $P < 0.05$; ***, $P < 0.001$.

the penetration of dyes in the tumor. Second, the oxygenation of these hypoxic tumor models was substantially increased after the treatment. Interestingly, the opening of the tumor vascular bed was observed over the whole tumor, as shown by both perfusion studies. This observation is consistent with the diffusion of BoNT-A in tissues. It was previously shown, using radiolabeled BoNT-A in animal models, that the toxin remains in the tissue injected, diffusing over a depth of 7 mm from the injection site (28). This diffusion is even larger in humans when using larger volumes for the injection (29). The practical consequence was that the injection in two discrete sites was sufficient to affect the whole vascular bed of this tumor model, whose volume was <1 cm^3 at the time of the treatment. From the oximetry study, we also learned that the opening of the vascular bed was sufficient to improve the oxygen supply of the tumor, enabling these hypoxic tumor models to increase their pO_2 from a radioresistant level to a radiosensitive level (below and above 5 mm Hg, respectively; refs. 18, 30). Moreover, this increase in tumor oxygenation was prolonged because the effect was already observed 1 day after the injection of BoNT-A and increased up to 3 days after the treatment.

To show the relevance of these findings for the treatment outcome, we carried out radiotherapy and chemotherapy experiments using suboptimal doses of the cytotoxic treatments. The response of the tumors was remarkably higher when the tumors received BoNT-A 3 days before the cytotoxic anticancer treatments. At this stage, our study consists of a proof-of-principle that the modulation of the vasoreactivity of the tumor vessels is a powerful strategy to increase the response to common anticancer treatments. Moreover, because BoNT-A is widely used in the clinic with a long-term established absence of toxicity (absence of systemic effect) when used appropriately (31), it is certainly valid to envision clinical trials with local administration of BoNT-A in easily accessible tumors to assess the relevance of the present study in human tumors. It should be emphasized that the dosage used in the present study is well within the range of dosage used in humans (1-100 units/kg). Interestingly, defining the issue of therapeutic gain using BoNT-A should not be a major source of concern. A potential clinical advantage of the combination of a sensitizing agent and radiation can only be foreseen if the potentiation of radiation response is higher in tumors than in normal tissues in the radiation field, indicating that the therapeutic ratio of the combined treatment is above unity. Classically, several normal tissue models are used to determine the whether an agent is responsible for toxicity on early responding tissue (e.g., intestinal regenerated crypt assay) or late responding tissues (e.g., leg contracture assay). However, in the case of BoNT-A, these assays are unlikely necessary as BoNT-A is administered directly inside the tumor with a very limited diffusion in the surrounding normal tissues. Even in this case, a radiosensitizing property on the normal tissue is unlikely as we showed that BoNT-A acts via an oxygen effect. Consequently, the radiosensitizing property will more than likely be higher for hypoxic tumor regions than for well-oxygenated tissues.

In summary, we have established that local administration of BoNT-A in the tumor significantly increases the tumor perfusion and oxygenation, most probably through an inhibition of neurotransmitter release and neurogenic contraction. We further showed that the opening of the vascular bed induced by BoNT-A offers a way to substantially increase the response of tumors to radiotherapy and chemotherapy. Further

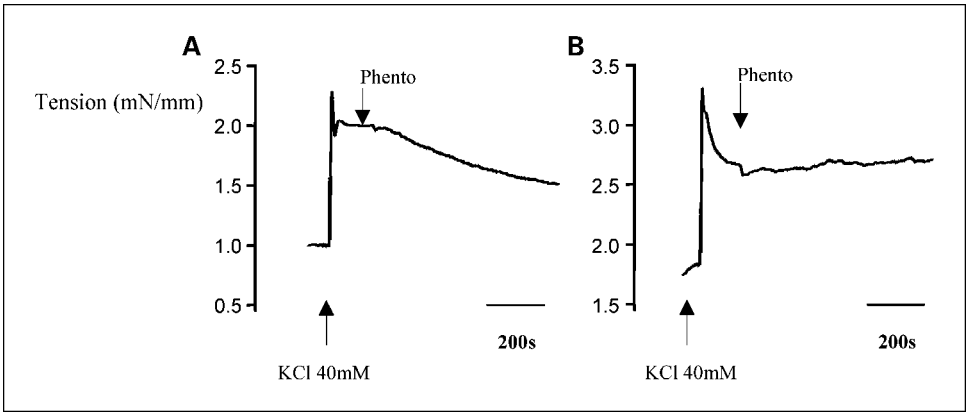

Fig. 9. Effect of BoTN-A on the relaxation to phentolamine. Representative tracings showing the relaxation of preconstricted co-opted saphenous arteries to phentolamine in the presence (*B*) or the absence (*A*) of BoTN-A treatment.

work is required to assess the usefulness in humans of this novel strategy to alleviate the resistance of tumors to cytotoxic treatments.

Acknowledgments

We thank Guerbet Laboratories (Roissy, France) for providing P792.

References

1. Feron O. Targeting the tumor vascular compartment to improve conventional cancer therapy. Trends Pharmacol Sci 2004;25:536–42.
2. Carmeliet P, Jain RK. Angiogenesis in cancer and other diseases. Nature 2000;407:249–57.
3. Thorpe PE. Vascular targeting agents as cancer therapeutics. Clin Cancer Res 2004;10:415–27.
4. Fayette J, Soria JC, Armand JP. Use of angiogenesis inhibitors in tumour treatment. Eur J Cancer 2005;41:1109–16.
5. Kaanders JH, Bussink J, van der Kogel AJ. ARCON: a novel biology-based approach in radiotherapy. Lancet Oncol 2002;3:728–37.
6. Padera TP, Stoll BR, Tooredman JB, Capen D, Di Tomaso E, Jain RK. Cancer cells compress intratumor vessels. Nature 2004;427:695.
7. Jain RK. Normalization of tumor vasculature: an emerging concept in antiangiogenic therapy. Science 2005;307:58–62.
8. Ansiaux R, Baudelet C, Jordan BF, et al. Thalidomide radiosensitizes tumors through early changes in the tumor microenvironment. Clin Cancer Res 2005;11:743–50.
9. Winkler F, Kozin SV, Tong RT, et al. Kinetics of vascular normalization by VEGFR2 blockade governs brain tumor response to radiation: role of oxygenation, angiopoietin-1, and matrix metalloproteinases. Cancer Cell 2004;6:553–63.
10. Brin MF, Hallett M, Jankovic J. Scientific and therapeutic aspects of Botulinum toxin. New York (USA): Lippincott Williams and Wilkins; 2002. p. 507.
11. Morris JL, Jobling P, Gibbins IL. Differential inhibition by botulinum neurotoxin A of cotransmitters released from autonomic vasodilator neurons. Am J Physiol Heart Circ Physiol 2001;281:H2124–32.
12. Morris JL, Jobling P, Gibbins IL. Botulinum neurotoxin A attenuates release of norepinephrine but not NPY from vasoconstrictor neurons. Am J Physiol Heart Circ Physiol 2002;283:H2627–35.
13. Rehman S, Jayson GC. Molecular imaging of antiangiogenic agents. Oncologist 2005;10:92–103.
14. Gallez B, Jordan B, Baudelet C, Misson PD. Pharmacological modifications of the partial pressure of oxygen in tumors. Evaluation using *in vivo* EPR oximetry. Magn Reson Med 1999;42:627–30.
15. Gallez B, Baudelet C, Jordan BF. Assessment of tumor oxygenation by electron paramagnetic resonance: principles and applications. NMR Biomed 2004;17:240–62.
16. Volpe JP, Hunter N, Basic I, Milas L. Metastatic properties of murine sarcomas and carcinomas. I. Positive correlation with lung colonization and lack of correlation with s.c. tumor take. Clin Exp Metastasis 1985;3:281–94.
17. Taper HS, Woolley GW, Teller MN, Lardis MP. A new transplantable mouse liver tumor of spontaneous origin. Cancer Res 1966;26:143–8.
18. Jordan BF, Grégoire V, Demeure RJ, et al. Insulin increases the sensitivity of tumors to irradiation: involvement of an increase in tumor oxygenation mediated by a nitric oxide dependent decrease of the tumor cells oxygen consumption. Cancer Res 2002;62:3555–61.
19. Baudelet C, Ansiaux R, Jordan BF, Havaux X, Macq B, Gallez B. Physiological noise in murine solid tumours using T2*-weighted gradient-echo imaging: a marker of tumour acute hypoxia? Phys Med Biol 2004;49:3389–411.
20. Galbraith SM, Maxwell RJ, Lodge MA, et al. Combretastatin A4 phosphate has tumor antivascular activity in rat and man as demonstrated by dynamic magnetic resonance imaging. J Clin Oncol 2003;21:2831–42.
21. Rogers DF, Boschetto P, Barnes PJ. Plasma exudation. Correlation between Evans blue dye and radiolabeled albumine in guinea pig airways *in vivo*. J Pharmacol Methods 1989;21:309–15.
22. Bradford M. A rapid and sensitive method for the quantitation of microgram quantities of protein utilizing the principle of dye-binding. Anal Biochem 1976;72:248–54.
23. Graff BA, Bjornaes I, Rofstad EK. Macromolecule uptake in human melanoma xenografts: relationships to blood supply, vascular density, microvessel permeability and extracellular volume fraction. Eur J Cancer 2000;36:1433–40.
24. Morris JL, Jobling P, Gibbins IL. Botulinum neurotoxin A attenuates release of norepinephrine but not NPY from vasoconstrictor neurons. Am J Physiol Heart Circ Physiol 2002;283:H2627–35.
25. Whall CW, Jr., Havlik RJ, Halpern W, Bohr DF. Potassium depolarization of adrenergic varicosities in resistance arteries from SHR and WKY rats. Blood Vessels 1983;20:23–33.
26. Sonveaux P, Dessy C, Martinive P, et al. Endothelin-1 is a critical mediator of myogenic tone in tumor arterioles: implications for cancer treatment. Cancer Res 2004;64:3209–14.
27. Sonveaux P, Dessy C, Brouet A, et al. Modulation of the tumor vasculature functionality by ionizing radiation accounts for tumor radio-sensitization and promotes gene delivery. FASEB J 2002;16:1979–81.
28. Tang-Liu DDS, Aoki KR, Dolly JO, et al. Intramuscular injection of ^{125}I-botulinum neurotoxin-complex versus ^{125}I-botulinum-free neurotoxin: time course of tissue distribution. Toxicon 2003;42:461–9.
29. Hsu TSJ, Dover JS, Arndt KA. Effect of volume and concentration on the diffusion of Botulinum exotoxin A. Arch Dermatol 2004;140:1351–4.
30. Jordan BF, Sonveaux P, Feron O, et al. Nitric oxide as a radiosensitizer: evidence for an intrinsic role in addition to its oxygen effect on oxygen delivery and consumption. Int J Cancer 2004;109:768–73.
31. Klein AW. Complications, adverse reactions, and insights with the use of botulinum toxin. Dermatol Surg 2003;29:549–56.